



Chance and necessity in the pleiotropic consequences of adaptation for budding yeast

Elizabeth R. Jerison^{1,2,4}, Alex N. Nguyen Ba², Michael M. Desai^{1,2}  and Sergey Kryazhinskiy³ 

Mutations that a population accumulates during evolution in one ‘home’ environment may cause fitness gains or losses in other environments. Such pleiotropic fitness effects determine the evolutionary fate of the population in variable environments and can lead to ecological specialization. It is unclear how the pleiotropic outcomes of evolution are shaped by the intrinsic randomness of the evolutionary process and by the deterministic variation in selection pressures across environments. Here, to address this question, we evolved 20 replicate populations of the yeast *Saccharomyces cerevisiae* in 11 laboratory environments and measured their fitness across multiple conditions. We found that evolution led to diverse pleiotropic fitness gains and losses, driven by multiple types of mutations. Approximately 60% of this variation is explained by the home environment of a clone and the most common parallel genetic changes, whereas about 40% is attributed to the stochastic accumulation of mutations whose pleiotropic effects are unpredictable. Although populations are typically specialized to their home environment, generalists also evolved in almost all of the conditions. Our results suggest that the mutations that accumulate during evolution incur a variety of pleiotropic costs and benefits with different probabilities. Thus, whether a population evolves towards a specialist or a generalist phenotype is heavily influenced by chance.

Populations adapt by accumulating mutations that are beneficial in their current environment, along with linked hitchhiker mutations¹. If a population finds itself in a new environment, the effects of previously accumulated mutations may change, potentially conferring fitness benefits or incurring fitness costs in the new condition. Such by-product (pleiotropic) effects of adaptation in one condition on fitness in others can expand the ecological niche of the organism^{2–4}, lead to ecological specialization and speciation^{4–6}, and help to maintain genetic and phenotypic diversity in populations^{7,8}. Fitness trade-offs can also be exploited for practical purposes, for example, to create attenuated antiviral vaccines⁹ or to slow down the evolution of multi-drug resistance¹⁰. However, despite decades of research, we still lack a fundamental understanding of the statistical structure of pleiotropy, especially for new mutations^{3,6–8,11–14}. That is, how do mutations that arise and reach high frequencies in a population adapting to one condition typically affect fitness of the population in other conditions?

To explain widespread ecological specialization and local adaptation in nature, pleiotropy was originally assumed to be mostly antagonistic, such that fitness benefits in one environment must come at a cost in others^{15–17}. However, recent field studies have found that locally adaptive alleles confer pleiotropic fitness defects much less frequently than anticipated^{8,12–14,18}. Although ecological specialization and local adaptation can arise without trade-offs^{19–21}, it is also possible that field studies provide a skewed view of the structure of pleiotropy owing to statistical complications and confounding factors, such as migration and unknown environmental variation^{22–24}.

Laboratory microbial and viral populations are powerful model systems in which the structure of pleiotropy can be investigated under controlled conditions and with a degree of replication seldom achievable in natural systems^{25–44} (reviewed recently in refs. 13,14,21). Experimental studies generally support the conclusions from the field that fitness trade-offs exist^{25–28,30–39,41,44,45} but are not

ubiquitous^{29,31,33,36,40,42,43,46}. However, why generalists or specialists evolve in different evolution experiments is not entirely clear^{13,18,36}. One possibility is that adaptation to each home environment leads to the accumulation of mutations that have typical, home-environment-dependent pleiotropic fitness effects, such that the pleiotropic outcomes of evolution depend primarily on the differences in selection pressures between environments^{36,41}. The set of home and non-home environments then determines whether specialists or generalists evolve in each specific case.

It is also possible that chance events have an important role^{13,33,36}. As independently evolving populations stochastically acquire different sets of mutations that could have dramatically different pleiotropic effects¹³, even populations evolving in the same condition may reach pleiotropically different states. Thus, in addition to differences in selection pressures between environments, random chance may determine whether a population evolves towards a specialist or a generalist phenotype.

Disentangling and quantifying the contributions of selection and chance to pleiotropy requires observing evolution in many replicate populations and measuring their fitness in many other conditions. To this end, we evolved populations of the yeast *S. cerevisiae* in a variety of laboratory environments, sequenced their full genomes and measured the fitness of the evolved clones in multiple panels of non-home conditions. To quantify the contribution of natural selection and evolutionary stochasticity to pleiotropy, we estimated the variance in the pleiotropic fitness gains and losses explained by these two factors. We also examined how pleiotropic outcomes depend on the similarity between the new and the home environments.

Results

To investigate the pleiotropic consequences of adaptation, we experimentally evolved 20 replicate *S. cerevisiae* populations in 11 different laboratory environments (a total of 220 populations). Each

¹Department of Physics, Harvard University, Cambridge, MA, USA. ²Department of Organismic and Evolutionary Biology, Harvard University, Cambridge, MA, USA. ³Division of Biological Sciences, University of California San Diego, La Jolla, CA, USA. ⁴Present address: Department of Physics, Stanford University, Stanford, CA, USA. ✉e-mail: mdesai@oeb.harvard.edu; skryazhi@ucsd.edu

Table 1 | Environmental conditions used in this study

Environment	Evolution condition	Measurement panels				Formulation
		Diagnostic	Salt	pH	Temp	
SC	✓	✓	✓	✓	✓	SC + 2% Glu, 30 °C
Low salt	✓		✓			SC + 2% Glu + 0.2 M NaCl, 30 °C
Med salt			✓			SC + 2% Glu + 0.4 M NaCl, 30 °C
High salt	✓	✓	✓			SC + 2% Glu + 0.8 M NaCl, 30 °C
pH 3	✓	✓		✓		SC + 2% Glu, buffered to pH 3, 30 °C
pH 3.8	✓			✓		SC + 2% Glu, buffered to pH 3.8, 30 °C
pH 6	✓			✓		SC + 2% Glu, buffered to pH 6, 30 °C
pH 7.3	✓	✓		✓		SC + 2% Glu, buffered to pH 7.3, 30 °C
Low temp	✓	✓			✓	SC + 2% Glu, 21 °C
Med temp					✓	SC + 2% Glu, 34 °C
High temp	✓	✓			✓	SC + 2% Glu, 37 °C
Low Glu	✓	✓				SC + 0.07% Glu, 30 °C
Gal	✓	✓				SC + 2% Gal, 30 °C

SC, synthetic complete medium; Med, medium; temp, temperature; Glu, glucose; Gal, galactose.

population was founded from a single colony that was isolated from a common clonal stock of a laboratory strain. We chose the 11 laboratory environments to represent various degrees of several types of physiological stresses (such as osmotic stress and temperature stress). A complete list of all 11 evolution conditions, in addition to two conditions used only for assays, is provided in Table 1.

We evolved each population in batch culture at an effective size of about $N_e \approx 2 \times 10^5$ for about 700 generations using our standard methods for laboratory evolution (see Methods). Seven populations were lost owing to pipetting errors during evolution, leaving a total of 213 evolved lines. We randomly selected a single clone from each evolved population for further analysis.

Specialization is the typical outcome of adaptation. To understand how adaptation to one home environment alters the fitness of the organism in other non-home environments, we measured the competitive fitness of each evolved clone relative to their common ancestor across multiple conditions (see Methods). We first focused on a diagnostic panel of eight conditions that represent different types of physiological stresses (see Table 1).

Figure 1 shows the median change in fitness of these clones across the eight diagnostic conditions. As expected, clones that evolved in all of the environments typically gained fitness in their home environment, although the magnitude of these gains varied between conditions (Fig. 1, diagonal entries). We quantified the degree of specialization as the average fraction of non-home environments in which clones lost fitness relative to their ancestor (see Methods). Figure 1 (left) shows that, by this definition, populations that evolved in all of the environments typically specialized to various degrees (for example, compare the populations that evolved at pH 3 with the populations that evolved at low temperature).

For the long-term survival of an ecological specialist, its fitness in the home environment must be greater than the fitness of populations that evolved elsewhere. To test whether adaptation leads to a 'resident' population that is fitter than 'invader' populations that evolved elsewhere, we estimated the proportion of pairwise competitions between residents and invaders in which the resident wins (see Methods). We found that, in most home environments, an average resident is able to outcompete most or all invaders from other environments (Fig. 1, bottom). The exception to this rule was the pH 3 environment, in which residents lost in more than half of competitions.

We conclude that adaptive evolution typically leads populations to specialize to their home environment, and the evolved specialists are typically able to resist invasions from populations that evolved elsewhere. As expected, the specific set of conditions in which an evolved population gains and loses fitness depends on the home environment of the population. One exception, which we discuss below, is the unexpected similarity between pleiotropic consequences of evolution in three apparently unrelated conditions—adaptation to high salt, pH 3 and pH 7.3 led to similar and large median fitness losses in synthetic complete medium (SC), galactose (Gal) and at low temperature.

Evolution leads to diverse but environment-specific pleiotropic outcomes. The patterns of median fitness gains and losses shown in Fig. 1 may be driven by differences in selection pressure between environments, such that mutations acquired in different environments have systematically different pleiotropic effects in other conditions. Alternatively, these patterns could have arisen because different clones stochastically acquired different sets of mutations with idiosyncratic patterns of fitness variation across environments.

To discriminate between these two possibilities, we quantified the variation in the patterns of pleiotropic fitness gains and losses. We calculated the pleiotropic profile of each clone—the eight-dimensional vector containing its fitness changes (relative to the ancestor) in the eight diagnostic environments. If clones isolated from the same home environment cluster together in this eight-dimensional space, it would indicate that evolution in this environment leaves a stereotypical pleiotropic signature. Lack of clustering would suggest that the patterns in the median pleiotropic profiles shown in Fig. 1 are driven by evolutionary stochasticity and idiosyncratic pleiotropy.

To visualize the clustering of pleiotropic profiles, we used *t*-stochastic nearest neighbour embedding (*t*-SNE) to project the eight-dimensional profiles onto two dimensions (Fig. 2a,b). This *t*-SNE embedding is useful in looking for cluster structure because it minimally distorts the original local distances between points, such that clones that are close together in the two-dimensional embedding have similar eight-dimensional pleiotropic profiles (in contrast to principal components analysis, for which this may not always be the case). In Fig. 2d, we show the patterns of pleiotropy that are associated with each of the measured clones. The colour of each clone in Fig. 2d is consistent with its colour in Fig. 2b.

The *t*-SNE embedding reveals that there are two large and clearly separated clusters, both of which contain clones from all of the home environments (Fig. 2a). The main features that discriminate between the two clusters are the fitness in SC, Gal and at low temperature (Fig. 2b,d). Clones that belong to one cluster lost 10–40% in these conditions, whereas clones that belong to the other cluster did not (Fig. 2b,d). We refer to these two phenotypes as V^- and V^+ , respectively, for reasons that we describe in the section ‘The genetic basis of pleiotropic outcomes’.

Clones that evolved in different conditions are not distributed identically in the *t*-SNE space. First, clones from different home environments have different likelihoods of evolving the V^- phenotype (χ^2 , $P=6.8 \times 10^{-8}$), for example, high temperature versus Gal-evolved clones. In fact, this variation explains the large median fitness losses in the SC, Gal and low-temperature conditions that we observed in Fig. 1 (Extended Data Fig. 1). Second, within the large V^+ and V^- clusters, clones from some environments form tight smaller clusters (for example, high-salt clones; Fig. 2a). More generally, 2.8 out of the 5 nearest neighbours of a typical clone are from the same environment, compared with 0.60 ± 0.12 under random permutation.

We next set out to quantify the extent to which the observed variation in pleiotropic profiles is explained by the deterministic differences in selection pressures between environments versus the intrinsic randomness of the evolutionary process. Using a nested linear model, we estimated the fractions of observed variance in fitness in each diagnostic environment that is attributed to the identity of the home environment of a clone and to measurement noise. We attribute the remaining unexplained variance to evolutionary stochasticity, that is, the fact that each clone acquired a unique set of mutations that have idiosyncratic pleiotropic effects. We found that the home environment accounts for 20–51% of the variance in fitness, depending on the diagnostic environment (Fig. 2c). Measurement noise accounts for less than 4% of variance, leaving 48–77% attributable to evolutionary stochasticity (Fig. 2c). If the status of a clone with respect to the V^+/V^- phenotype becomes known (for example, after measuring its fitness at low temperature), the fraction of unexplained variance decreases to 16–70% (Fig. 2c).

Taken together, these observations show that the home environment leaves a distinct signature in the pleiotropic profile of a clone, such that clones that evolve in the same condition tend to be more similar to each other than clones that evolve in different conditions. However, these deterministic differences are generally less important than the randomness of the evolutionary process, accounting for on average 34% of the variance in pleiotropic outcomes, compared with 65% for stochastic effects.

The genetic basis of pleiotropic outcomes. Next, we sought to determine the genetic basis that underlies the diverse pleiotropic outcomes that we observed above using two approaches. First, we used DNA staining and flow cytometry (see Methods) to look for ploidy changes, because this is a common mode of adaptation in yeast^{47–51}. Second, we sequenced the full genomes of the evolved clones. We performed these analyses on all 213 clones, that is, those evolved in the diagnostic conditions considered above as well as other intermediate-stress environments listed in Table 1. In 15 cases, sequencing failed at the library preparation stage or due to insufficient coverage, leaving us with 198 sequenced clones. Using standard bioinformatic methods for calling SNPs and small indels (see Methods), we identified a total of 1,925 de novo mutations. We note that, because our sequencing and analysis pipeline can result in false negatives (that is, certain mutations are difficult to confidently identify), our results represent a subset of all of the mutations in each sequenced clone.

Loss of killer virus causes the V^- phenotype. We began by looking for the genetic differences between the V^+ and V^- clones. We found no association between V^+ or V^- phenotypes and ploidy or

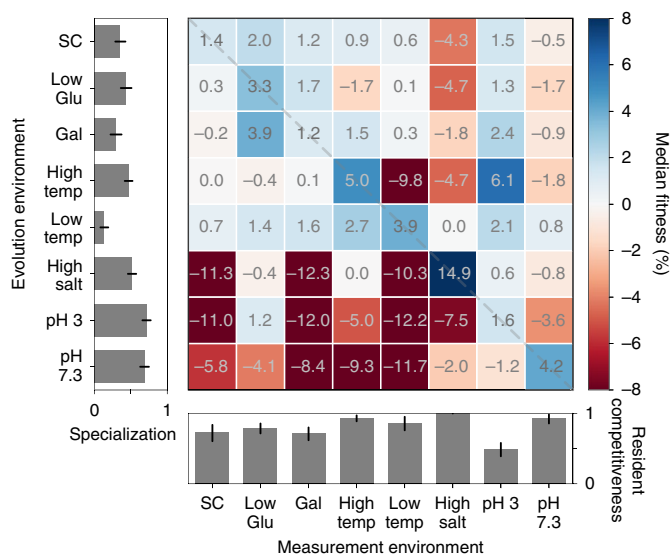


Fig. 1 | Fitness gains and losses in diagnostic conditions after evolution in each condition. Each square shows the median fitness gain or loss in a measurement environment (columns) across all of the populations evolved in a given home environment (rows) for ~700 generations. Left, the degree of specialization after evolution in each home environment. The degree of specialization is defined as the average proportion of measurement environments in which clones lost fitness relative to the ancestor. Bottom, the competitiveness of a resident clone in its home environment against invasions from other environments. The competitiveness is defined as the average proportion of evolved clones from other environments that are less fit than a randomly chosen resident clone. The error bars represent 95% confidence intervals bootstrapped over clones in each evolution condition.

any of the mutations identified in the sequencing data. Instead, multiple lines of evidence demonstrate that the V^- phenotype was caused by the loss of the yeast killer virus, a toxin–antitoxin system encoded by a ~2-kb cytoplasmic double-stranded RNA^{52–56} that was present in the ancestor of our experiment (and was retained in the V^+ clones). First, we found that both the ancestor and 7 out of 7 randomly selected V^+ clones displayed the killer-virus band in a gel electrophoresis assay (see Methods), whereas all of the 7 randomly selected V^- clones did not (Fig. 3a). Second, we competed the evolved clones against the reference strain that was cured of the killer virus (see Methods). We performed this assay at low temperature because V^- clones have the largest fitness defect in this condition in competitions against their direct virus-carrying ancestor (Fig. 2d). As expected, this severe fitness defect entirely disappeared in competitions against the cured ancestor (Fig. 3b). We obtained several additional pieces of evidence that support the conclusion that the loss of the killer virus is the cause of the V^- phenotype (see Methods; Supplementary Figs. 1 and 2).

Our results suggest that the severe fitness defects in the SC, low temperature and Gal environments (Figs. 1 and 2d) are not due to an inherent growth disadvantage. Rather, V^- clones suffer large losses of fitness in competitions against the virus-carrying ancestor because they succumb to the virus expressed by the ancestor. As a consequence, these fitness losses are frequency dependent (Extended Data Fig. 2); they are particularly severe in the SC, low temperature and Gal conditions probably because virus activity is higher in these conditions⁵⁷. Nevertheless, virus loss evolved even in these environments (Fig. 2d). This initially puzzling observation could be explained if the virulence of the virus was lost first and resistance was lost second, after non-virulent genotypes dominated the population. In support of this explanation, we found that

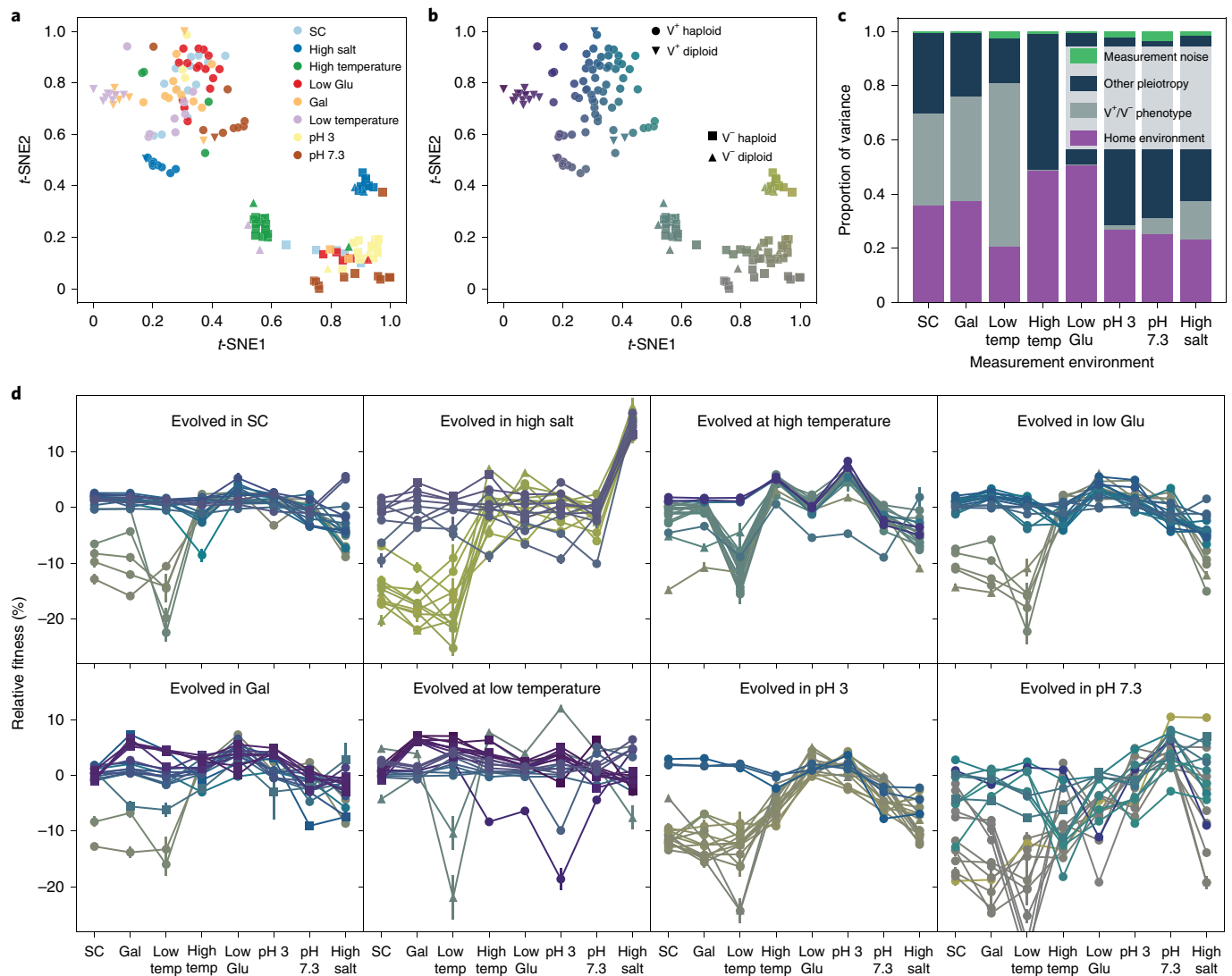


Fig. 2 | Environmental and stochastic determinants of pleiotropic profiles. **a**, *t*-SNE dimensional reduction of the pleiotropic profiles. Each point represents a clone; the eight-dimensional vector of clone fitness across the eight conditions was projected onto two dimensions using *t*-SNE. Clones are coloured according to home environment. **b**, *t*-SNE projection as described in **a**. The colours are assigned on the basis of the *t*-SNE coordinates to establish visual correspondence between this projection and the full pleiotropic profiles shown in **d**. **c**, Proportion of the variance in clone fitness in each environment that is attributable to (in this order) home environment, V⁺/V⁻ phenotype, other pleiotropy (unexplained variance) and measurement noise. Clones are excluded from their own home environment. **d**, The pleiotropic profiles of clones from each home environment. Profiles are coloured as in **b**. The error bars represent ± 1 s.e.m. on clone fitness.

some of the evolved clones have similar fitness relative to both the virus-carrying and virus-cured ancestors (Fig. 3b, horizontal lines), suggesting that they are resistant but non-virulent⁵⁸. A recent study examining the co-evolution of yeast and its killer virus also reported such stepwise progression towards virus loss and showed that virus loss probably provides no fitness benefit to the host⁵⁹.

Diversity at the genetic level underlies diversity of pleiotropic outcomes.

We next looked for the genetic basis of the fine-scale phenotypic variation between clones that we observed in our *t*-SNE plot (Fig. 2a,b). We found that 35 out of 213 clones became diploid during evolution. Diploid clones evolved more often in some environments than in others (χ^2 , $P = 1.3 \times 10^{-4}$) and 24 out of 35 diploid clones retained the killer virus, whereas 11 lost the killer virus (Fig. 2b). Moreover, 13 V⁺ diploid clones that evolved in the low temperature and Gal conditions formed a small cluster in the *t*-SNE space (Fig. 2a, inverted triangles), suggesting that a change in ploidy—irrespective of where

it evolved—leads to certain characteristic changes in the pleiotropic profile, perhaps in conjunction with other mutations.

We next used our full-genome sequencing data to call putatively beneficial SNPs and indels. We identified such mutations as non-synonymous, nonsense or frameshift changes within multi-hit genes, which we define here as genes that were mutated in four or more clones across all of the home environments, or in two or more clones from the same home environment (see Methods; Supplementary Fig. 3). In total, we identified 176 such mutations in 42 multi-hit genes (Fig. 4a). Only three individual multi-hit genes (*SIR3*, *HNM1* and *PDE2*) were significantly associated with one home environment ($P < 0.01$, Bonferroni-corrected permutation test; see Methods). Mutations in other multi-hit genes arose in multiple home environments, but with significantly different frequencies ($P < 10^{-4}$; see Methods; Fig. 4a).

To quantify the extent to which this genetic information improves our ability to statistically predict the fitness of a clone in a diagnostic

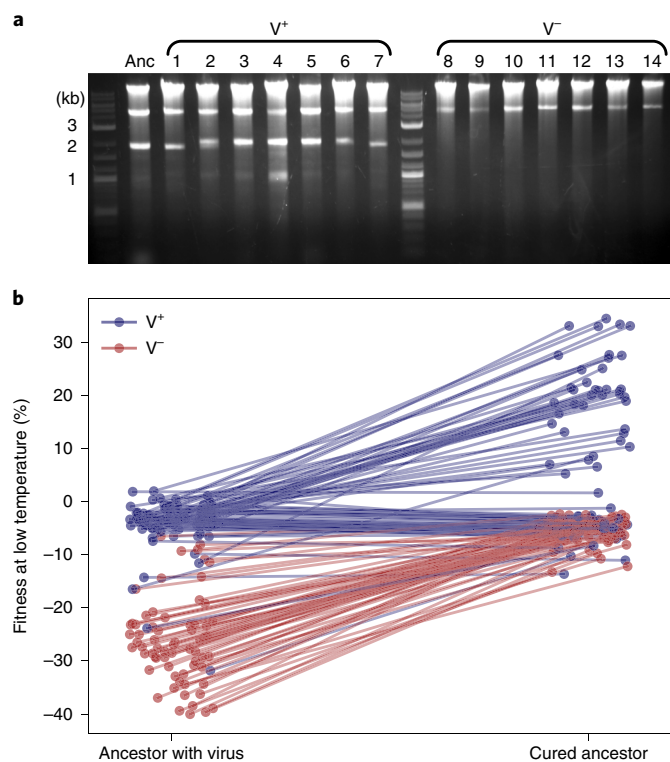


Fig. 3 | The V^- phenotype is caused by the loss of yeast killer virus. **a, Gel electrophoresis of total DNA and double-stranded RNA extracted from 15 clones. Anc is the common ancestor of the experiment; evolved clones 1–7 are from the V^+ cluster (Fig. 2b), that is, without a fitness defect at 21°C; evolved clones 8–14 are from the V^- cluster, that is, with a fitness defect at 21°C. The top (~4 kb) band is consistent with the helper virus, and the bottom (~2 kb) band is consistent with the killer virus. **b**, Fitness of all of the evolved clones relative to the ancestor and to the ancestor cured of the killer virus. Classification of clones into V^+ (blue) and V^- (red) is based on the t -SNE plot shown in Fig. 2b.**

environment, we expanded the list of predictor variables in the nested linear model described in the previous section to include the presence or absence of multi-hit mutations shown in Fig. 4a and the ploidy status. We found that mutations in multi-hit genes account for 11–30% of the variance in pleiotropic effects (Fig. 4b), and all of the genetic factors combined account for 17–77% of variance. After accounting for these genetic factors, the home environment of a clone still explains 5–35% of variance. This implies that, even though mutations in some genes fail to meet the multi-hit-gene significance threshold, they nevertheless have predictable pleiotropic effects. We found that 15–60% of variance remains unexplained, and we now attribute it to the accumulation of mutations with unpredictable pleiotropic effects.

In summary, multiple types of genetic changes accumulate during evolution in all of our environments. Genetic changes at the same loci occur in populations that evolved in different environments, but with different rates. As a result, the genotype of a clone at a few loci explains about half of the variation in its pleiotropic profile. A clone's genotype and home environment together, on average, explain approximately 60% of this variation. The remaining ~40% are attributed to the stochastic accumulation of mutations of which pleiotropic effects are unpredictable.

Fitness trade-offs are not inevitable, but their frequency increases with dissimilarity between environments. We next sought to understand what determines whether a clone that evolved in one

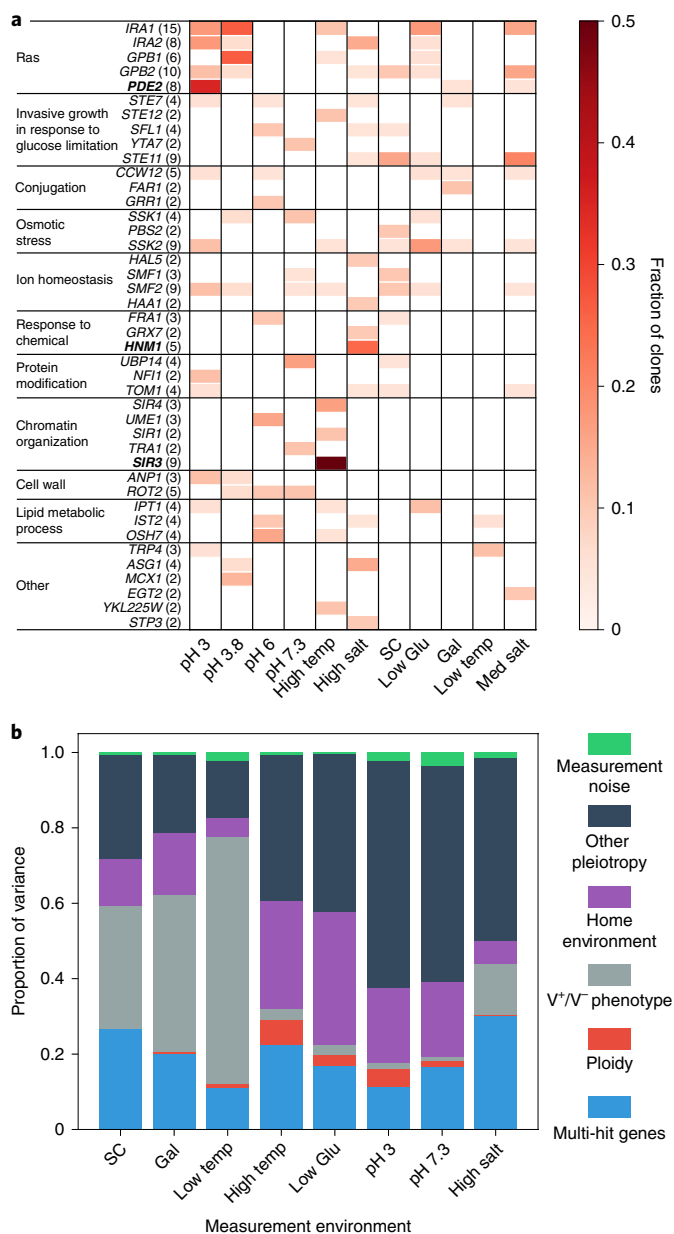


Fig. 4 | Mutations across evolution conditions and genetic determinants of pleiotropy. **a**, Genes with four or more non-synonymous mutations across the experiment, or two or more within one home environment, organized into the Ras pathway and thereafter by the Gene Ontology (GO) Slim process. The number in the parentheses next to each gene name indicates the total number of detected non-synonymous mutations in that gene. Genes indicated in bold are significantly associated with one home environment. **b**, The proportion of variance in clone fitness in each environment attributable (in this order) to mutations in multi-hit genes, ploidy, V^+/V^- phenotype, home environment (beyond these previously listed factors), other pleiotropy (unexplained variance) and measurement noise. Clones were excluded from their own home environment. Only clones evolved in diagnostic conditions were considered in this analysis, as described in Fig. 2.

condition gains or loses fitness in another. Our hypothesis is that the pleiotropic outcomes depend on the dissimilarity between the test condition and the clone's home environment^{36,42}. As it is unclear how to measure similarity among conditions in our original diagnostic panel, we tested this hypothesis in three additional panels of

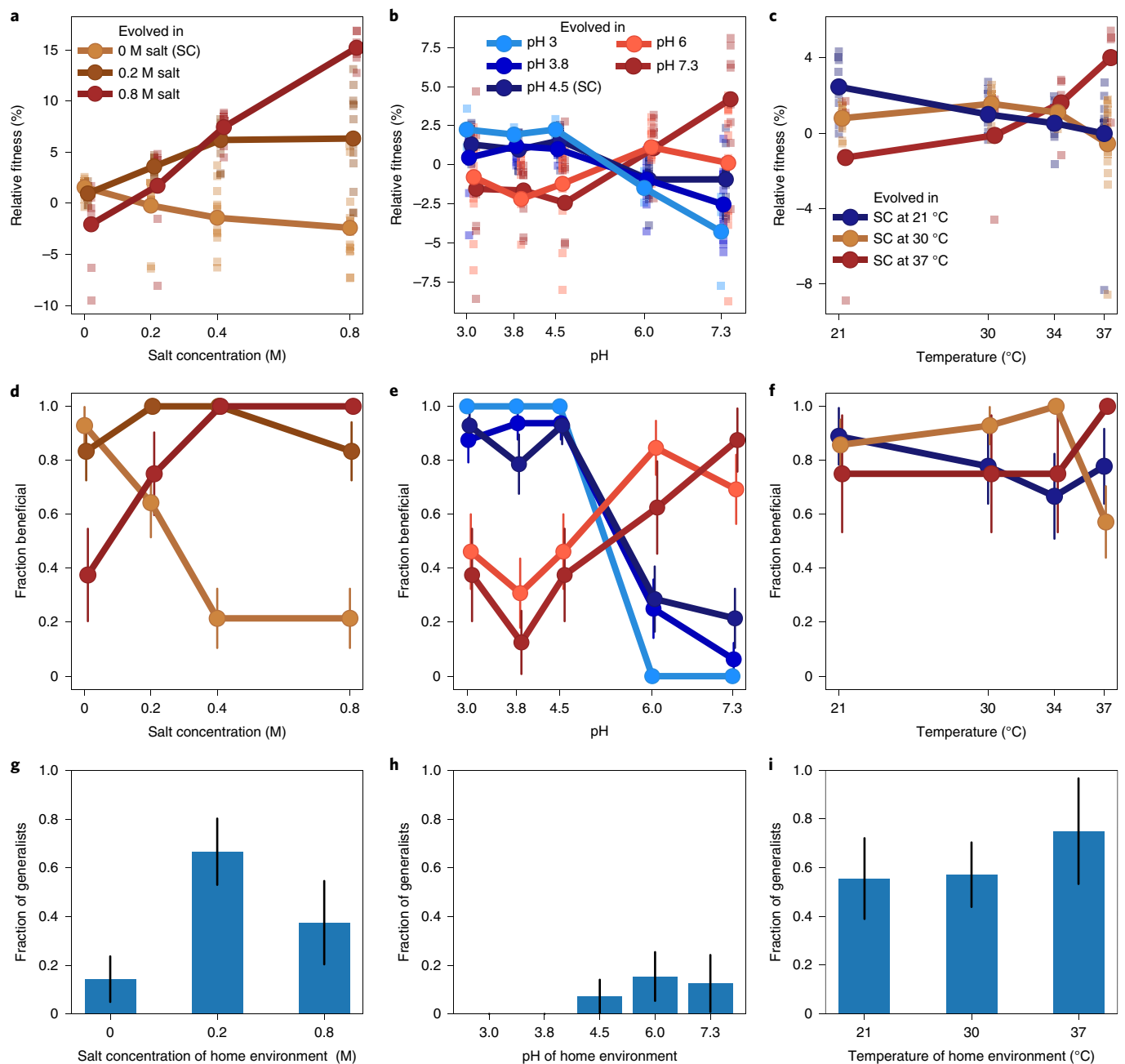


Fig. 5 | Specialization across salt, pH and temperature panels of environments. a–c, Average fitness of clones from each home environment (colours) across the following test conditions: salt concentration (a), pH (b) and temperature (c). The squares represent the fitness of individual clones. Note that in b, two measurements that fell below -10% are not displayed (one clone evolved at pH 6 and was measured at pH 3.8, and one clone evolved at pH 7.3 and was measured at pH 4.5). **d–f,** The fraction of clones from each home environment (colours) that gained fitness in the following test conditions: salt concentration (d), pH (e) and temperature (f). The error bars represent ± 1 s.e. **g–i,** The fraction of clones from each home environment (salt concentration (g), pH (h) and temperature (i)) that gained fitness across all of the test conditions in the panel. The error bars represent ± 1 s.e.

environments, in which yeast is exposed to different intensities of a particular type of physiological stress (salt, temperature and pH; see Table 1). To simplify interpretation, we restricted this analysis to V^+ haploid clones (see Methods).

Consistent with results for the diagnostic panel (Fig. 1, Extended Data Fig. 1), clones typically gained more fitness in their home environment than clones that evolved in other conditions in the same panel (Fig. 5a–c). The mean fitness of a clone was lower in conditions that were more dissimilar to its home environment, consistent with our hypothesis. Higher moments of the distribution of

pleiotropic outcomes might also depend on the similarity between conditions, but the patterns are less clear (Extended Data Fig. 3).

The fact that clones that evolved at one extreme of a panel lost fitness on average at the other extreme suggests that there may be inherent physiological trade-offs between fitness in dissimilar environments. However, we found that many clones that evolved at one extreme of each panel actually gained fitness at the other extreme (Fig. 5d–f). The only exceptions were the clones that evolved in the more acidic environments—all of which lost fitness in the most basic conditions (Fig. 5b,e). However, some of the clones

that evolved in the more basic environments gained fitness in the more acidic conditions, suggesting that mutations beneficial at both extremes are available. In fact, generalists—clones of which fitness increased across the entire panel—arose in almost all of the environments (Fig. 5g–i).

These results demonstrate that mutations exist that are beneficial across the entire range of environments that vary along one physicochemical axis. Thus, the trade-offs between fitness, even in the most dissimilar conditions along such axis, are not physiologically inevitable. To further corroborate this conclusion, we measured the correlation between the fitness of clones in pairs of environments in each panel (Extended Data Figs. 4–6). If fitness trade-offs between a pair of conditions were physiologically inevitable, we would expect a negative correlation between fitness measured in these conditions. Instead, we observed diverse and complex fitness covariation patterns, but there is a notable lack of strong negative correlations between clone fitness even in the most dissimilar pairs of environments. In conclusion, our results suggest that whether a population evolves towards being a specialist or a generalist depends on the specific set of mutations that it accumulates, that is, this outcome is largely stochastic.

Discussion

To assess how chance and necessity in evolution affect the fitness of an organism across multiple environments, we evolved populations of budding yeast in a variety of laboratory home conditions. We characterized each population by its pleiotropic profile—the vector of fitness gains and losses in an array of diagnostic environments. We found that a diverse set of pleiotropic profiles arose during evolution in all of the home conditions. Underlying this phenotypic diversity, we found a diversity of evolutionary outcomes at the genetic level. Nevertheless, home environments leave statistically distinct signatures in the genome that, in turn, lead to statistically distinct pleiotropic profiles for clones evolved in different conditions. We estimated that a clone's home environment and the set of most common genetic changes together explain about 60% of variance in the pleiotropic fitness gains and losses of the clone. The remaining ~40% are attributable to evolutionary stochasticity, that is, the accumulation of hitchhikers or rare beneficial variants of which pleiotropic effects are unpredictable.

Despite the fact that the pleiotropic outcomes of evolution in any individual population are to a large degree governed by chance, clear and repeatable patterns emerge when we consider ensembles of populations that evolved in the same home environment. On average, evolution leads to specialization such that pleiotropic fitness gains are typically smaller or turn into losses in environments that are less similar to the home environment (Fig. 5). The most obvious explanation for these patterns is that different environments exert different selection pressures on the organism, but variations in the spectra and rates of mutations across environments may also have a role⁶⁰.

Our results help us to better understand the evolution of specialists and generalists, a long-standing problem in evolutionary ecology^{11,21,61}. To explain the ubiquity of specialists, many models require physiological trade-offs or antagonistic pleiotropy^{15,18,61}. By contrast, it has long been appreciated that fitness losses in non-home environments can arise without physiological trade-offs if the population accumulates mutations that are neutral in the home environment and deleterious elsewhere^{19,42}. However, field and experimental studies to date do not clearly favour one model over another^{3,8,12,13}.

To explain the existing data, Bono et al. recently proposed a model that unifies the antagonistic pleiotropy and mutation accumulation perspectives¹³. In their model, the fitness effects of mutations form a continuum, such that the mutations accumulated in the home environment may provide a range of pleiotropic fitness

costs and benefits in a non-home condition (see figure 1 in ref. ¹³). If mutations that incur pleiotropic costs are more common and/or more beneficial than those that provide pleiotropic benefits, the population will tend to lose fitness in the non-home condition and evolve into a specialist. Our results are consistent with this model. Moreover, they indicate that the probabilities of acquiring mutations with various pleiotropic effects depend on the similarity between conditions. As the physicochemical similarity between conditions declines, more mutations that are beneficial in one become deleterious in the other. As a result, populations are more likely to suffer pleiotropic fitness costs in conditions that are more dissimilar to the home environment.

Here we examined the statistics of pleiotropy among mutations that arose in populations of a particular size descended from one particular ancestral yeast genotype. These statistics probably depend on the population size, because populations of different size sample different sets of adaptive mutations⁶². Furthermore, different genotypes probably have access to beneficial mutations with different statistics of pleiotropy⁶³. To understand these broader patterns, we need to know the joint distribution of the fitness effects of new mutations and how this distribution varies across genotypes.

Assuming that the structure of pleiotropy does not change substantially between closely related genotypes, our results suggest that longer periods of evolution in a constant environment should lead to further specialization, simply because pleiotropically costly mutations are more abundant and generalists have no advantage. In nature, most populations live in fluctuating environments in which generalist mutations are favoured by selection. Why then do 'jacks of all traits' not evolve? Our results suggest that generalist genotypes may not be physiologically impossible but are simply unlikely to evolve because mutations that are beneficial in increasingly larger sets of distinct conditions become exceedingly rare.

Methods

Experimental evolution. The *S. cerevisiae* strain yGIL104 (derived from W303, genotype *MATa, URA3, leu2, trp1, CAN1, ade2, his3, bar1Δ::ADE2* (ref. ⁶⁴)) was used to found 220 populations for evolution. Each population was founded from a single colony that was picked from an agar plate. The populations were propagated in batch culture in 96-well polystyrene plates (Corning, VWR, 29445-154), with 128 μl of medium per well. Populations evolving in the same environment were grown in wells B2–B11 and E2–E11 on the same plate. Except for the Gal and low-glucose conditions, all medium contained 2% dextrose (BD, VWR, 90000-904), 0.67% Yeast Nitrogen Base (YNB) with nitrogen (Sunrise Science, 1501-500) and 0.2% Synthetic Complete Medium (SC; Sunrise Science, 1300-030). The Gal condition contained 2% Gal (Sigma-Aldrich, G0625) instead of dextrose, and the low-glucose condition contained 0.07% dextrose. Other conditions contained the following in addition to SC complete: low salt, 0.2 M sodium chloride; medium salt, 0.4 M sodium chloride; high salt, 0.8 M sodium chloride; pH 3, 0.02 M disodium phosphate and 0.04 M citric acid; pH 3.8, 0.0354 M disodium phosphate and 0.032 M citric acid; pH 6, 0.0642 M disodium phosphate and 0.0179 M citric acid; and pH 7.3, 0.0936 M disodium phosphate and 0.00032 M citric acid. Buffered medium was filter sterilized; all other media were autoclaved.

All of the populations were grown at 30 °C, except for the high-temperature lines (37 °C) and the low-temperature lines (room temperature (21 ± 0.5 °C)). In the SC, high-temperature, medium-salt, low-glucose, pH 3, pH 3.8 and pH 6 conditions, dilutions were carried out once every 24 h. In the Gal, low-temperature and high-salt conditions, dilutions were performed every 36 h. All dilutions were performed using a Biomek-FX pipetting robot (Beckman-Coulter). Before each transfer, cells were resuspended by shaking on a Titramax 100 orbital plate shaker at 1,200 r.p.m. for at least 1 min. In the pH 7.3 condition, dilutions were performed every 48 h. At each transfer, all of the populations were diluted 1:512 except for the low-glucose populations, which were diluted 1:64. This maintained a bottleneck size of about 10⁴ cells in all of the conditions. Populations underwent approximately the following numbers of generations (doublings): SC, high temperature, medium salt: 820; low glucose: 730; pH 3, pH 3.8 and pH 6: 755; and high salt, low temperature: 612. Every seven transfers, populations were mixed with glycerol to a final concentration 25% (w/v) and stored at –80 °C. Each 96-well plate contained blank wells; no contamination of blank wells was observed during the evolution. Over the course of evolution, 7 populations were lost owing to pipetting errors, leaving 213 evolved lines.

To pick clones for further analysis, each final population was streaked onto SC-complete medium with 2% agar. One colony per population was picked, grown in 128 μ l of SC at 30°C, mixed with 25% (w/v) glycerol and stored at -80°C.

Competitive fitness assays. We conducted flow-cytometry-based competitive fitness assays against yGIL104-cit, a fluorescently labelled derivative of the common ancestor, yGIL104. To construct the fluorescent reference strain, we amplified the HIS3MX6-ymCitrineM233I construct from genomic DNA of strain yJHK111 (courtesy of M. Muller, J. Koschwanez and A. Murray, Department of Molecular and cellular Biology, Harvard University) using the primers oGW137 and oGW138 and integrating it into the his3 locus. The fitness effect of the fluorescent marker is less than 1% in all of the environments (Supplementary Fig. 5).

Fitness assays were conducted as described previously^{65,66}. In brief, we grew all of the test strains and the reference strain from frozen stock in SC medium at 30°C. After 24 h, we diluted all of the lines into the assay environment for one growth cycle of preconditioning. We then mixed the reference strain and the test strains 50/50. We monitored the relative numbers of the reference and test strain over 3 d in co-culture. We measured fitness as $s = \frac{1}{\tau} \ln \left(\frac{n_{tr}}{n_{tr} n_{tr}} \right)$ where τ is the number of generations between timepoints, n_{tr} is the count of the test strain at the initial timepoint, n_{tr} is the count of the test strain at the final timepoint, and n_{tr} and n_{tr} are the counts for the reference. Fitness gains and losses are reported per 700 generations of evolution.

Library preparation and whole-genome sequencing. Libraries were prepared for sequencing as described previously⁶⁷. In brief, genomic DNA was extracted from each of the 213 clones using the PureLink Pro 96 Genomic Purification Kit (Life Technologies, K1821-04A) and quantified using the Qubit platform. The multiplexed sequencing library for the Illumina platform was prepared using the Nextera kit (Illumina, FC-121-1031 and FC-121-1012) and a modified version of the Illumina-recommended protocol⁶⁷. Libraries were sequenced on a Nextera Hi-seq 2500 in rapid-run mode with paired-end 150-bp reads.

Nucleic acid staining for ploidy. Clones were grown to saturation in YPD (2% dextrose, 2% peptone and 1% yeast extract). Saturated cultures were diluted 1:10 into 120 μ l of sterile water in a 96-well plate. The plate was centrifuged and cultures were resuspended in 50 μ l of fresh water. Then, 100 μ l of ethanol was added to each well, and the wells were mixed slowly. Plates were incubated for 1 h at room temperature or overnight at 4°C. Cells were centrifuged, ethanol solution was removed and 65 μ l RNase solution added (2 mg ml⁻¹ RNase in 10 mM Tris-HCl, pH 8.0 and 15 mM NaCl). The samples were incubated at 37°C for 2 h. To stain, 65 μ l of 300 nM SYTOX green (Thermo Fisher Scientific, S-34860) in 10 mM Tris-HCl was added to each well, for a final volume of 130 μ l. The plates were incubated at room temperature in foil for 20 min.

Fluorescence was measured using flow cytometry on a Fortessa analyzer (FITC channel). Fluorescence peaks were compared to known haploid and diploid controls to score ploidy. For 19 out of 213 clones, we observed smeared peaks intermediate between the haploid and diploid peaks; we called these clones as undetermined and included them with the haploids in analysis.

SNP and indel identification. We called SNPs and small indels as described previously⁶⁸, with the following two modifications. First, we aligned reads to a custom W303 reference genome⁶⁹. Second, for clones called as diploid on the basis of staining, we called mutations as heterozygous if they occurred at frequencies between 0.4 and 0.8, and otherwise as homozygous. We called mutations in all other clones if they occurred at a frequency of at least 0.8. We included both heterozygous and homozygous mutations in subsequent analyses.

For 95.4% (1,925) of the mutations that we called, the mutation was found in one clone (that is, the mutation was unique at the nucleotide level). The remaining 4.6% (88) of mutations were found in two or more clones. These mutations may have originated from standing genetic variation in the starting strain, and we therefore excluded them from our analysis of de novo mutations.

Analysis of genetic parallelism. To test for parallelism at the gene level, we redistributed the observed non-synonymous mutations across the genes in the yeast genome, under a multinomial distribution with probabilities proportional to the gene lengths. We determined that genes with four non-synonymous mutations across the experiment, or two non-synonymous mutations within one evolution condition, were enriched (Supplementary Fig. 3). To divide these genes into categories, we first classified genes as belonging to the Ras pathway on the basis of de novo mutations in the same pathway found in previous studies^{49,69}. We classified the remainder of the genes using GO Slim 'biological process' analysis, placing genes into GO Slim categories in order of the process enrichment score.

To test for associations between individual multi-hit genes and home environments, we redistributed the observed mutations in each gene across environments, preserving the number of mutations per gene and the number of mutations per environment, but ignoring which mutations occurred in which

clones. We calculated the nominal P value by comparing the maximum number of hits to a particular gene in any environment in the permuted and original data. To correct for multiple testing, we multiplied the obtained nominal P value by the total number of genes (Bonferroni correction).

We used a mutual-information-based test statistic to test for overall association between the evolution environments and mutated genes. We defined the mutual information as:

$$M = \sum_{i=1}^n p_i \sum_{j=1}^m \left(p_{ij} \log_2 \frac{p_{ij}}{p_j} + (1 - p_{ij}) \log_2 \frac{1 - p_{ij}}{1 - p_j} \right) \quad (1)$$

where m is the number of significant genes, n is the number of evolution environments, p_j is the probability of a clone from environment i having a mutation in gene j , p_i is the probability of any clone having a mutation in gene j and p_i is the probability that a clone evolved in environment i . By convention, $p_j \log_2(p_j) = 0$ if $p_j = 0$ and probabilities were estimated on the basis of the observed frequencies of the events. We determined significance by comparing M to the null distribution under permutation, preserving the number of mutations per gene and the number of mutations per environment. For the null distribution, M was 0.67 (0.62–0.73), whereas, for the data, M was 1.15. The code used for analysis and figure generation is available at: <https://github.com/erjerison/pleiotropy>. The number of sequenced clones from each environment was: SC (19), high salt (20), high temperature (18), low Glu (17), Gal (18), low temperature (18), pH3 (17), pH7.3 (18), pH6 (19), pH3.8 (15) and medium salt (19).

t-SNE and clustering analysis. We used the sklearn.manifold.t-SNE class in the Python package scikit-learn 0.2, with 2 dimensions and perplexity 30, to project the eight-dimensional fitness vectors into a two-dimensional t-SNE space. We then used the sklearn.cluster.KMeans class to perform k -means clustering with $k = 2$ in the t-SNE space. We used this cluster assignment to call V^+ and V^- phenotypes. These clusters correspond to those that are identifiable visually in Fig. 2. The number of clones from each diagnostic environment was as follows: SC (19), high salt (20), high temperature (20), low Glu (20), Gal (19), low temperature (19), pH3 (18) and pH7.3 (20).

Specialization and competitiveness summary statistics. To assess the degree of specialization of a clone, we counted the number of non-home environments in which the fitness of the clone relative to its ancestor was 2 s.e.m. below zero. Fig. 1 (left) shows the proportion of such conditions averaged over all of the clones from the same home environment. To assess the competitiveness of resident clones in their home environment relative to clones evolved elsewhere, we estimated the proportion of all of the clones evolved in other conditions with fitness lower than a randomly chosen resident clone (Fig. 1, bottom). For both statistics, we measured 95% confidence intervals on the basis of a bootstrap over clones in each evolution environment.

Nested linear models for analysis of variance. To evaluate the fraction of the variance in pleiotropic effects attributable to the evolution condition versus stochastic evolutionary effects, we fit the following series of nested linear models for each of the diagnostic measurement conditions:

$$Y_i = \alpha + \sum_j \beta_j E_{ij} + \epsilon_i, \quad (2)$$

$$Y_i = \alpha + \sum_j \beta_j E_{ij} + \gamma V_i + \epsilon_i \quad (3)$$

where Y_i is the fitness of clone i ; $E_{ij} = 1$ if clone i evolved in environment j , 0 otherwise; $V_i = 1$ if clone i is V^+ , 0 otherwise; ϵ_i is the measurement noise, α , β_j and γ are the regression coefficients. Note that we excluded clones from their own home environment to focus on pleiotropic effects, as opposed to adaptation to the home condition. Note also that we restricted analysis to clones measured in all eight diagnostic conditions to maintain comparability between environments. We fit the models using the sklearn.linear_model.LinearRegression class in Python, and used the score method of this class to calculate R^2 .

Fig. 2c shows the partitioning of the total variance in Y_i as follows. We measured the variance due to measurement error as:

$$V = \frac{1}{n} \sum_{i=1}^n \frac{V_i}{n_r} \quad (4)$$

where n is the number of clones, n_r is the number of replicate measurements of each clone and V_i is the estimate of the variance across replicate fitness measurements of clone i . We attribute the variance explained by model (2) to home environment. We attribute the variance not explained by model (2) but explained by model (3) to V^+ / V^- phenotype. We attributed leftover variance not accounted for by model (3) and not attributed to measurement noise to additional stochastic effects, which we label other pleiotropy.

To evaluate the contributions of most common genetic factors to the pleiotropic effects (Fig. 4b), we performed an analogous analysis of variance using the following series of nested linear models:

$$Y_i = \alpha + \sum_j m_j M_{ij} + \epsilon_i \quad (5)$$

$$Y_i = \alpha + \sum_j m_j M_{ij} + \delta D_i + \epsilon_i \quad (6)$$

$$Y_i = \alpha + \sum_j m_j M_{ij} + \delta D_i + \gamma V_i + \epsilon_i \quad (7)$$

$$Y_i = \alpha + \sum_j m_j M_{ij} + \delta D_i + \gamma V_i + \sum_j \beta_j E_{ij} + \epsilon_i \quad (8)$$

where $M_{ij} = 1$ if clone i has at least 1 mutation in biological process j out of 10 biological processes shown in Fig. 4a (other than 'Other'); $D_i = 1$ if clone i is a diploid, 0 otherwise; δ is a regression coefficient.

Extraction of double-stranded RNA and gel electrophoresis. Yeast cell pellets from 1.5 ml of an overnight culture were resuspended in 50 μ l of a Zymolyase-based enzymatic digest to lyse the cells (5 mg ml⁻¹ Zymolyase 20T, 100 mM sodium phosphate buffer pH 7.4, 10 mM EDTA, 1 M sorbitol, 20 mM dithiothreitol, 200 μ g ml⁻¹ RNase A, 0.5% 3-(*N,N*-dimethylmyristylammonio)propanesulfonate) and incubated at 37°C for 1 h. The sphaeroplasted cells were then lysed with 200 μ l of lysis/binding buffer (4.125 M guanidine thiocyanate, 25% isopropanol, 100 mM MES pH 5). After vortexing briefly, the clear solution was passed through a standard silica column for DNA purification, and washed twice with 600 μ l of wash buffer (20 mM Tris-Cl pH 7.4, 80% ethanol). After drying the column, the DNA and double-stranded RNA were eluted using a low-salt elution buffer (10 mM Tris-Cl pH 8.5).

Total extracted genomic material was processed for standard gel electrophoresis (1% agarose gel, Tris-acetate-EDTA (TAE) running buffer, stained with 0.5 μ g ml⁻¹ ethidium bromide).

Curing the killer virus. Strain yGIL104-cit-V⁻ was constructed from yGIL104-cit as follows. yGIL104-cit was grown from frozen stock overnight in YPD. Saturated culture was diluted 1:10⁵ and 250 μ l was plated onto YPD. The plates were incubated at 39°C for 72 h. Colonies were picked and the presence of the virus double-stranded RNA band was tested as described above. Two out of nine colonies tested displayed the helper virus band but no killer virus band; seven out of nine retained both bands. The two V⁻ colonies were restreaked and a clone from each was grown in YPD, mixed with glycerol to 25% and stored at -80°C. Competitive fitness assays were performed with both clones against yGIL104 at several starting frequencies in the SC, 21°C, 37°C and high-salt conditions. The fitness of the two clones at each frequency and condition were the same, so one clone was designated yGIL104-cit-V⁻ and was used as a cured reference in all subsequent assays.

We used fitness relative to the original and cured ancestor to classify clones from the three environments that were not included in the diagnostic panel as either V⁺ or V⁻ (Supplementary Fig. 4). We also note that one clone (high-temperature clone 20) was lost from the cured reference fitness assay.

Additional experiments to determine the cause of the low-temperature fitness defects.

We performed several types of experiments to determine the genetic basis of the large observed fitness defects in the low-temperature environment. First, we reconstructed all six non-synonymous mutations called in one evolved clone with the fitness defect in the ancestral background. The strain background used for reconstructions was yERJ3, which was constructed from yGIL104 by amplifying the HIS3 construct from yGIL104-cit using primers 3 and 4, which target the URA3 locus. This construct was transformed into yGIL104 using standard techniques⁷⁰, plated on CSM-His dropout medium, and replica plated to 5-fluoroorotic acid (5FoA) and CSM-Ura to verify the His⁺/Ura⁻ phenotype.

We used the delitto perfetto method for the reconstructions⁷¹. In brief, we amplified a URA3-Hph construct from plasmid pMJM37 (provided by M. J. McDonald) using primers 6–17, which target the yeast genome 5 bp upstream and downstream of the mutations of interest. We selected on CSM-Ura and hygromycin B, picked two clones and transformed each with two complementary 90-bp repair oligos (18–29) containing the mutation of interest and the flanking genic region. We selected on 5FoA and replica plated to hygromycin to determine the phenotype. We used primers 30–41 to amplify the locus in the reconstructed line for Sanger sequencing.

We performed fitness assays of yERJ3, the reconstructed lines and the knockout intermediates against yGIL104-cit in the SC, 37°C, 21°C and high-salt conditions. For one mutation, in the gene *CUE4*, one reconstruction replicate displayed a significant fitness defect across all of the conditions, whereas the other replicate did not. We discarded this clone as a probable reconstruction artefact.

We note that the reconstruction background yERJ3 had an apparent fitness defect of a few percent in the high-salt environment, potentially due to the engineered URA3 auxotrophy. We report fitness of reconstructed lines relative

to yERJ3 in Supplementary Fig. 1. These mutations account for the fitness advantage in the clone's home environment (high salt), but none of them carry the characteristic large fitness defect at low temperature.

To determine whether the defect was caused by a mutation that we did not detect during sequencing, we back-crossed three evolved clones that displayed the defect to the common ancestor and picked four-spore complete tetrads. The strain yERJ10 (genotype *MAT α* yGIL104 ura3::HIS3) was constructed from yGIL104 as described above for yERJ3. The mating type was switched using an inducible Gal::HO plasmid, pAN216a-URA3-GAL::HO-Ste2pr::SkHIS3-Ste3pr::LEU2. The strain was transformed with the plasmid and plated on CSM-Ura dropout medium. A colony was grown in SC-Ura dropout medium with 2% sucrose overnight. Then, 1 ml of culture was centrifuged and resuspended in SG-Ura dropout medium (2% Gal) to induce. Cells were plated on SC-Leu dropout medium directly after transfer to SG-Ura and, 60 min later, colonies were streaked on SD complete + 5FoA to eliminate the plasmid. *MAT α* versions of evolved lines were constructed using the same method. After mating, diploids were selected on CSM-Ura-His dropout medium. Diploids were sporulated in Spo++ medium⁷⁰ supplemented with 0.5% dextrose at 21°C for 3–5 d. Tetrads were dissected according to standard yeast genetics methods⁷⁰. Four-spore complete tetrads from each mating were grown in SC, which was mixed with glycerol to final concentration 25% and frozen at -80°C. Fitness assays of four-spore complete tetrads from each mating, competed against yGIL104-cit, were conducted as described above at 21°C. We also constructed a mitochondrial-cured (ρ^-) version of the reference and of the evolved lines; the fitness of spores from crosses involving these lines were not distinguishable from the corresponding ρ^+ crosses, so spore fitness were pooled.

In Supplementary Fig. 2, we show data from a representative one of these crosses: yERJ10 *MAT α* \times High Salt-17 *MAT α* (backcross) and High Salt-17 *MAT α* \times High Salt-17 *MAT α* (control cross). We observed that the fitness defect did not segregate 2:2, as would be expected for a Mendelian trait; rather, very few of the segregants from the back-cross displayed the defect. This observation is consistent with a cytoplasmic genetic element (the virus) that is carried by one parent (the ancestor) but not the other (evolved line), and is usually reinherited by segregants after mating.

Given that the defect did not seem to be caused by a nuclear genetic mutation, we next addressed whether there was evidence of a direct interaction between strains during competition. To achieve this, we investigated whether the size of the fitness defect depended on the frequency of the competitors. In Extended Data Fig. 2, we show an example of such a competition experiment between the putative virus-carrying reference and the cured ancestor at low temperature. The strong frequency dependence of the fitness defect is consistent with secretion of a toxin by one competitor—the strain lacking the virus (and, therefore, the antitoxin) is at a larger disadvantage when the virus-carrying competitor is at high frequency.

Together with the direct observation of the virus band through gel electrophoresis and the competition of all of the evolved lines against the cured ancestor, as described in the Results section, these observations support the conclusion that the loss of the killer virus particle in some evolved lines caused the large fitness defect at low temperature.

Reporting Summary. Further information on research design is available in the Nature Research Reporting Summary linked to this article.

Data availability

The data used in Figs. 1, 2 and 5 are provided in Supplementary Table 1. The data used in Fig. 3 are provided in Supplementary Table 2. The data used in Fig. 4 are provided in Supplementary Tables 1 and 3. The sequences reported in this paper have been deposited in the BioProject database (accession number, PRJNA554163). All of the strains are available from the corresponding authors on request.

Code availability

The code used for analysis and figure generation is available at <https://github.com/erjerson/pleiotropy>.

Received: 2 August 2019; Accepted: 28 January 2020;
Published online: 9 March 2020

References

- Barrick, J. E. & Lenski, R. E. Genome dynamics during experimental evolution. *Nat. Rev. Genet.* **14**, 827–839 (2013).
- Lee, C. E. Evolutionary genetics of invasive species. *Trends Ecol. Evol.* **17**, 386–391 (2002).
- Bedhomme, S., Hillung, J. & Elena, S. F. Emerging viruses: why are not jacks of all trades? *Curr. Opin. Virol.* **10**, 1–6 (2015).
- Kassen, R. The experimental evolution of specialists, generalists, and the maintenance of diversity. *J. Evol. Biol.* **15**, 173–190 (2002).
- Schluter, D. Evidence for ecological speciation and its alternative. *Science* **323**, 737–741 (2009).
- Forister, M., Dyer, L. A., Singer, M., Stireman, J. O. III & Lill, J. Revisiting the evolution of ecological specialization, with emphasis on insect-plant interactions. *Ecology* **93**, 981–991 (2012).

7. Mitchell-Olds, T., Willis, J. H. & Goldstein, D. B. Which evolutionary processes influence natural genetic variation for phenotypic traits? *Nat. Rev. Genet.* **8**, 845–856 (2007).
8. Savolainen, O., Lascoux, M. & Merilä, J. Ecological genomics of local adaptation. *Nat. Rev. Genet.* **14**, 807–820 (2013).
9. Minor, P. D. Live attenuated vaccines: historical successes and current challenges. *Virology* **479**, 379–392 (2015).
10. Kim, S., Lieberman, T. D. & Kishony, R. Alternating antibiotic treatments constrain evolutionary paths to multidrug resistance. *Proc. Natl Acad. Sci. USA* **111**, 14494–14499 (2014).
11. Futuyma, D. J. & Moreno, G. The evolution of ecological specialization. *Annu. Rev. Ecol. Syst.* **19**, 207–233 (1988).
12. Anderson, J. T., Willis, J. H. & Mitchell-Olds, T. Evolutionary genetics of plant adaptation. *Trends Genet.* **27**, 258–266 (2011).
13. Bono, L. M., Smith, L. B. Jr, Pfennig, D. W. & Burch, C. L. The emergence of performance trade-offs during local adaptation: insights from experimental evolution. *Mol. Ecol.* **26**, 1720–1733 (2017).
14. Elena, S. F. Local adaptation of plant viruses: lessons from experimental evolution. *Mol. Ecol.* **26**, 1711–1719 (2017).
15. Levins, R. *Evolution in Changing Environments: Some Theoretical Explorations* (Princeton Univ. Press, 1968).
16. MacArthur, R. H. *Geographical Ecology: Patterns in the Distribution of Species* (Princeton Univ. Press, 1984).
17. Stearns, S. C. Trade-offs in life-history evolution. *Funct. Ecol.* **3**, 259–268 (1989).
18. Remold, S. Understanding specialism when the jack of all trades can be the master of all. *Proc. Natl Acad. Sci. USA* **279**, 4861–4869 (2012).
19. Kawecki, T. J. Accumulation of deleterious mutations and the evolutionary cost of being a generalist. *Am. Nat.* **144**, 833–838 (1994).
20. Whitlock, M. C. The red queen beats the jack-of-all-trades: the limitations on the evolution of phenotypic plasticity and niche breadth. *Am. Nat.* **148**, S65–S77 (1996).
21. Bono, L. M., Draghi, J. A. & Turner, P. E. Evolvability costs of niche expansion. *Trends Genet.* **36**, 14–23 (2019).
22. Anderson, J. T., Lee, C.-R., Rushworth, C. A., Colautti, R. I. & Mitchell-Olds, T. Genetic trade-offs and conditional neutrality contribute to local adaptation. *Mol. Ecol.* **22**, 699–708 (2013).
23. Ågren, J., Oakley, C. G., McKay, J. K., Lovell, J. T. & Schemske, D. W. Genetic mapping of adaptation reveals fitness tradeoffs in *Arabidopsis thaliana*. *Proc. Natl Acad. Sci. USA* **110**, 21077–21082 (2013).
24. Tiffin, P. & Ross-Ibarra, J. Advances and limits of using population genetics to understand local adaptation. *Trends Ecol. Evol.* **29**, 673–680 (2014).
25. Cooper, V. S. & Lenski, R. E. The population genetics of ecological specialization in evolving *Escherichia coli* populations. *Nature* **407**, 736–739 (2000).
26. Turner, P. E. & Elena, S. F. Cost of host radiation in an RNA virus. *Genetics* **156**, 1465–1470 (2000).
27. Zhong, S., Khodursky, A., Dykhuizen, D. E. & Dean, A. M. Evolutionary genomics of ecological specialization. *Proc. Natl Acad. Sci. USA* **101**, 11719–11724 (2004).
28. MacLean, R. C., Bell, G. & Rainey, P. B. The evolution of a pleiotropic fitness tradeoff in *Pseudomonas fluorescens*. *Proc. Natl Acad. Sci. USA* **101**, 8072–8077 (2004).
29. Ostrowski, E. A., Rozen, D. E. & Lenski, R. E. Pleiotropic effects of beneficial mutations in *Escherichia coli*. *Evolution* **59**, 2343–2352 (2005).
30. Duffy, S., Turner, P. E. & Burch, C. L. Pleiotropic costs of niche expansion in the RNA bacteriophage φ6. *Genetics* **172**, 751–757 (2006).
31. Bennett, A. F. & Lenski, R. E. An experimental test of evolutionary trade-offs during temperature adaptation. *Proc. Natl Acad. Sci. USA* **104**, 8649–8654 (2007).
32. Dettman, J. R., Sirjusingh, C., Kohn, L. M. & Anderson, J. B. Incipient speciation by divergent adaptation and antagonistic epistasis in yeast. *Nature* **447**, 585–588 (2007).
33. Lee, M.-C., Chou, H.-H. & Marx, C. J. Asymmetric, bimodal trade-offs during adaptation of *Methylobacterium* to distinct growth substrates. *Evolution* **63**, 2816–2830 (2009).
34. Wenger, J. W. et al. Hunger artists: yeast adapted to carbon limitation show trade-offs under carbon sufficiency. *PLoS Genet.* **7**, e1002202 (2011).
35. Jasmin, J.-N., Dillon, M. M. & Zeyl, C. The yield of experimental yeast populations declines during selection. *Proc. Natl Acad. Sci. USA* **279**, 4382–4388 (2012).
36. Jasmin, J.-N. & Zeyl, C. Evolution of pleiotropic costs in experimental populations. *J. Evol. Biol.* **26**, 1363–1369 (2013).
37. Yi, X. & Dean, A. M. Bounded population sizes, fluctuating selection and the tempo and mode of coexistence. *Proc. Natl Acad. Sci. USA* **110**, 16945–16950 (2013).
38. Hietpas, R. T., Bank, C., Jensen, J. D. & Bolon, D. N. Shifting fitness landscapes in response to altered environments. *Evolution* **67**, 3512–3522 (2013).
39. Hong, K.-K. & Nielsen, J. Adaptively evolved yeast mutants on galactose show trade-offs in carbon utilization on glucose. *Metab. Eng.* **16**, 78–86 (2013).
40. Rodríguez-Verdugo, A., Carrillo-Cisneros, D., González-González, A., Gaut, B. S. & Bennett, A. F. Different tradeoffs result from alternate genetic adaptations to a common environment. *Proc. Natl Acad. Sci. USA* **111**, 12121–12126 (2014).
41. Schick, A., Bailey, S. F. & Kassen, R. Evolution of fitness trade-offs in locally adapted populations of *Pseudomonas fluorescens*. *Am. Nat.* **186**, S48–S59 (2015).
42. Leiby, N. & Marx, C. J. Metabolic erosion primarily through mutation accumulation, and not tradeoffs, drives limited evolution of substrate specificity in *Escherichia coli*. *PLoS Biol.* **12**, e1001789 (2014).
43. McGee, L. W. et al. Payoffs, not tradeoffs, in the adaptation of a virus to ostensibly conflicting selective pressures. *PLoS Genet.* **10**, e1004611 (2014).
44. Fraebel, D. T. et al. Environment determines evolutionary trajectory in a constrained phenotypic space. *eLife* **6**, e24669 (2017).
45. Lalić, J., Cuevas, J. M. & Elena, S. F. Effect of host species on the distribution of mutational fitness effects for an RNA virus. *PLoS Genet.* **7**, e1002378 (2011).
46. Li, C. & Zhang, J. Multi-environment fitness landscapes of a tRNA gene. *Nat. Ecol. Evol.* **2**, 1025–1032 (2018).
47. Selmecki, A. M. et al. Polyploidy can drive rapid adaptation in yeast. *Nature* **519**, 349–352 (2015).
48. Gerstein, A. C., Chun, H.-J. E., Grant, A. & Otto, S. P. Genomic convergence toward diploidy in *Saccharomyces cerevisiae*. *PLoS Genet.* **2**, e145 (2006).
49. Venkataram, S. et al. Development of a comprehensive genotype-to-fitness map of adaptation-driving mutations in yeast. *Cell* **166**, 1585–1596 (2016).
50. Voordeckers, K. et al. Adaptation to high ethanol reveals complex evolutionary pathways. *PLoS Genet.* **11**, e1005635 (2015).
51. Harari, Y., Ram, Y. & Kupiec, M. Frequent ploidy changes in growing yeast cultures. *Curr. Genet.* **64**, 1001–1004 (2018).
52. Wickner, R. B. Double-stranded and single-stranded RNA viruses of *Saccharomyces cerevisiae*. *Annu. Rev. Microbiol.* **46**, 347–375 (1992).
53. Vagnoli, P., Musmanno, R. A., Cresti, S., DiMaggio, T. & Coratza, G. Occurrence of killer yeasts in spontaneous wine fermentations from the tuscany region of italy. *Appl. Environ. Microbiol.* **59**, 4037–4043 (1993).
54. Schmitt, M. J. & Breinig, F. Yeast viral killer toxins: lethality and self-protection. *Nat. Rev. Microbiol.* **4**, 212–221 (2006).
55. Greig, D. & Travisano, M. Density-dependent effects on allelopathic interactions in yeast. *Evolution* **62**, 521–527 (2008).
56. Pieczynska, M. D., de Visser, J. A. G. & Korona, R. Incidence of symbiotic dsRNA killer viruses in wild and domesticated yeast. *FEMS Yeast Res.* **13**, 856–859 (2013).
57. Kandel, J. S. in *Viruses of Fungi and Simple Eukaryotes* (eds Koltin, Y. & Leibowitz, M. J.) Ch. 11 (CRC Press, 1988).
58. Schmitt, M. J. & Breinig, F. The viral killer system in yeast: from molecular biology to application. *FEMS Microbiol. Rev.* **26**, 257–276 (2002).
59. Buskirk, S. W., Rokes, A. B. & Lang, G. I. Adaptive evolution of a rock-paper-scissors sequence along a direct line of descent. Preprint at [bioRxiv https://doi.org/10.1101/700302](https://doi.org/10.1101/700302) (2019).
60. Liu, H. & Zhang, J. Yeast spontaneous mutation rate and spectrum vary with environment. *Curr. Biol.* **29**, 1584–1591 (2019).
61. Sexton, J. P., Montiel, J., Shay, J. E., Stephens, M. R. & Slatyer, R. A. Evolution of ecological niche breadth. *Annu. Rev. Ecol. Evol. Syst.* **48**, 183–206 (2017).
62. Good, B. H., Rouzine, I. M., Balick, D. J., Hallatschek, O. & Desai, M. M. Distribution of fixed beneficial mutations and the rate of adaptation in asexual populations. *Proc. Natl Acad. Sci. USA* **109**, 4950–4955 (2012).
63. Tikhonov, M., Kachru, S. & Fisher, D. S. Modeling the interplay between plastic tradeoffs and evolution in changing environments. Preprint at [bioRxiv https://doi.org/10.1101/711531](https://doi.org/10.1101/711531) (2019).
64. Lang, G. I. & Murray, A. W. Estimating the per-base-pair mutation rate in the yeast *Saccharomyces cerevisiae*. *Genetics* **178**, 67–82 (2008).
65. Lang, G. I., Botstein, D. & Desai, M. M. Genetic variation and the fate of beneficial mutations in asexual populations. *Genetics* **188**, 647–661 (2011).
66. Kryazhimskiy, S., Rice, D. P., Jerison, E. R. & Desai, M. M. Global epistasis makes adaptation predictable despite sequence-level stochasticity. *Science* **344**, 1519–1522 (2014).
67. Baym, M. et al. Inexpensive multiplexed library preparation for megabase-sized genomes. *PLoS ONE* **10**, e0128036 (2015).
68. Jerison, E. R. et al. Genetic variation in adaptability and pleiotropy in budding yeast. *eLife* **6**, e27167 (2017).
69. Lang, G. I. et al. Pervasive genetic hitchhiking and clonal interference in forty evolving yeast populations. *Nature* **500**, 571–574 (2013).
70. Sherman, F., Fink, G. R. & Hicks, J. B. *Methods in Yeast Genetics: Laboratory Manual* (Cold Spring Harbor, 1981).
71. Storici, F., Lewis, L. K. & Resnick, M. A. In vivo site-directed mutagenesis using oligonucleotides. *Nat. Biotechnol.* **19**, 773–776 (2001).

Acknowledgements

We thank members of the Desai and Kryazhimskiy laboratories for experimental assistance and comments on the manuscript. M.M.D. acknowledges support from the Simons Foundation (grant no. 376196), NSF (grant no. DEB-1655960) and NIH

(grant no. GM104239). S.K. acknowledges support from the BWF Career Award at Scientific Interface (grant no. 1010719.01), the Alfred P. Sloan Foundation (grant no. FG-2017-9227) and the Hellman Foundation.

Author contributions

E.R.J., M.M.D. and S.K. designed the research. E.R.J., S.K. and A.N.N.B. performed experiments and analysis. E.R.J., M.M.D. and S.K. wrote the paper.

Competing interests

The authors declare no competing interests.

Additional information

Extended data is available for this paper at <https://doi.org/10.1038/s41559-020-1128-3>.

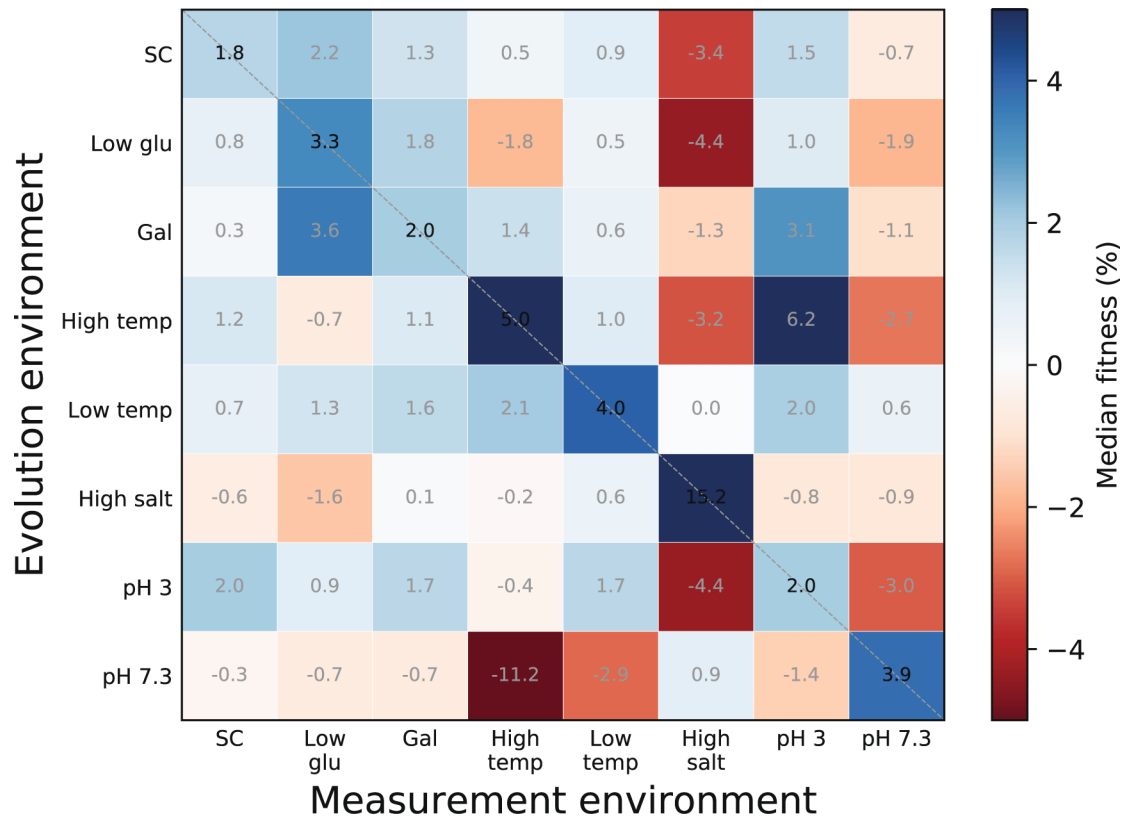
Supplementary information is available for this paper at <https://doi.org/10.1038/s41559-020-1128-3>.

Correspondence and requests for materials should be addressed to M.M.D. or S.K.

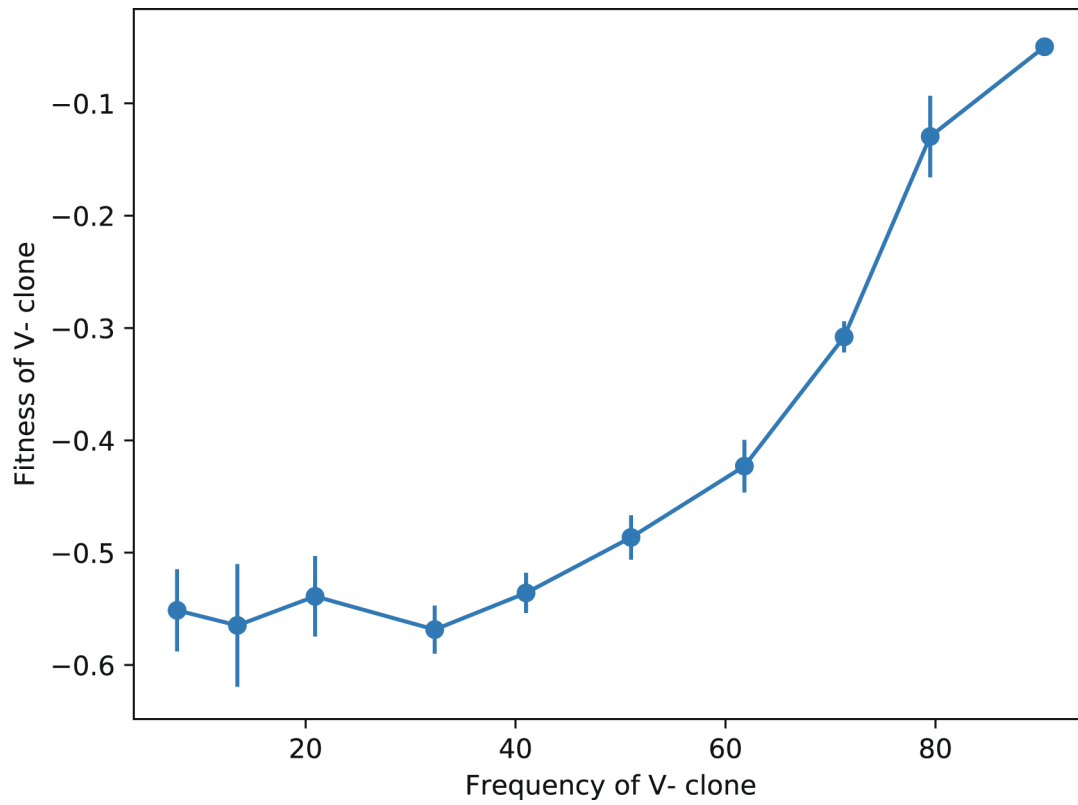
Reprints and permissions information is available at www.nature.com/reprints.

Publisher's note Springer Nature remains neutral with regard to jurisdictional claims in published maps and institutional affiliations.

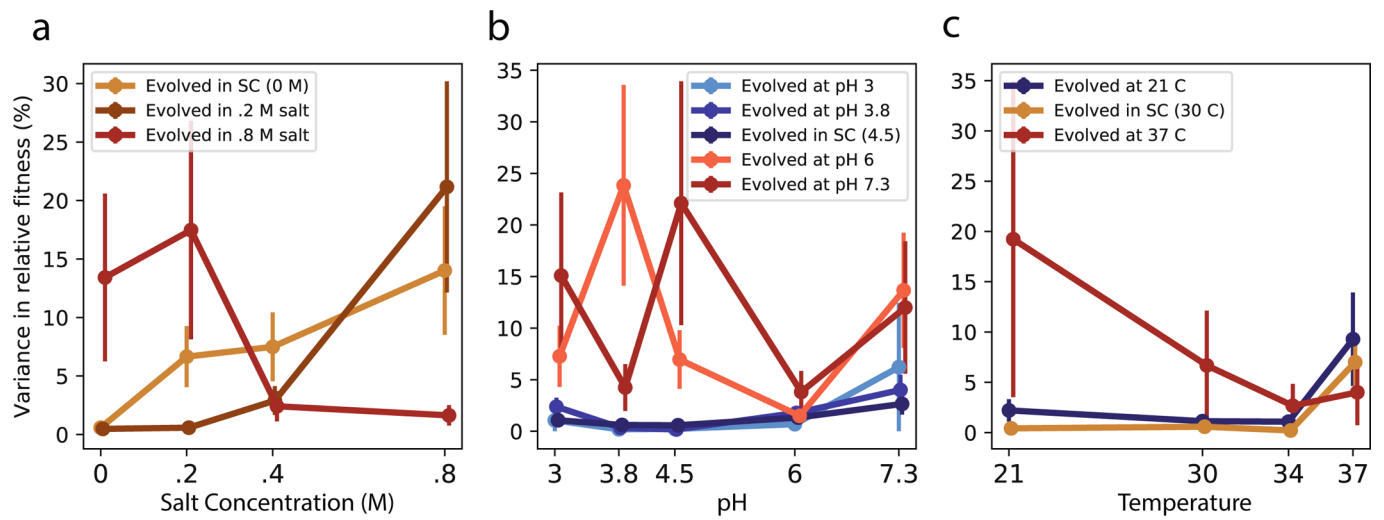
© The Author(s), under exclusive licence to Springer Nature Limited 2020



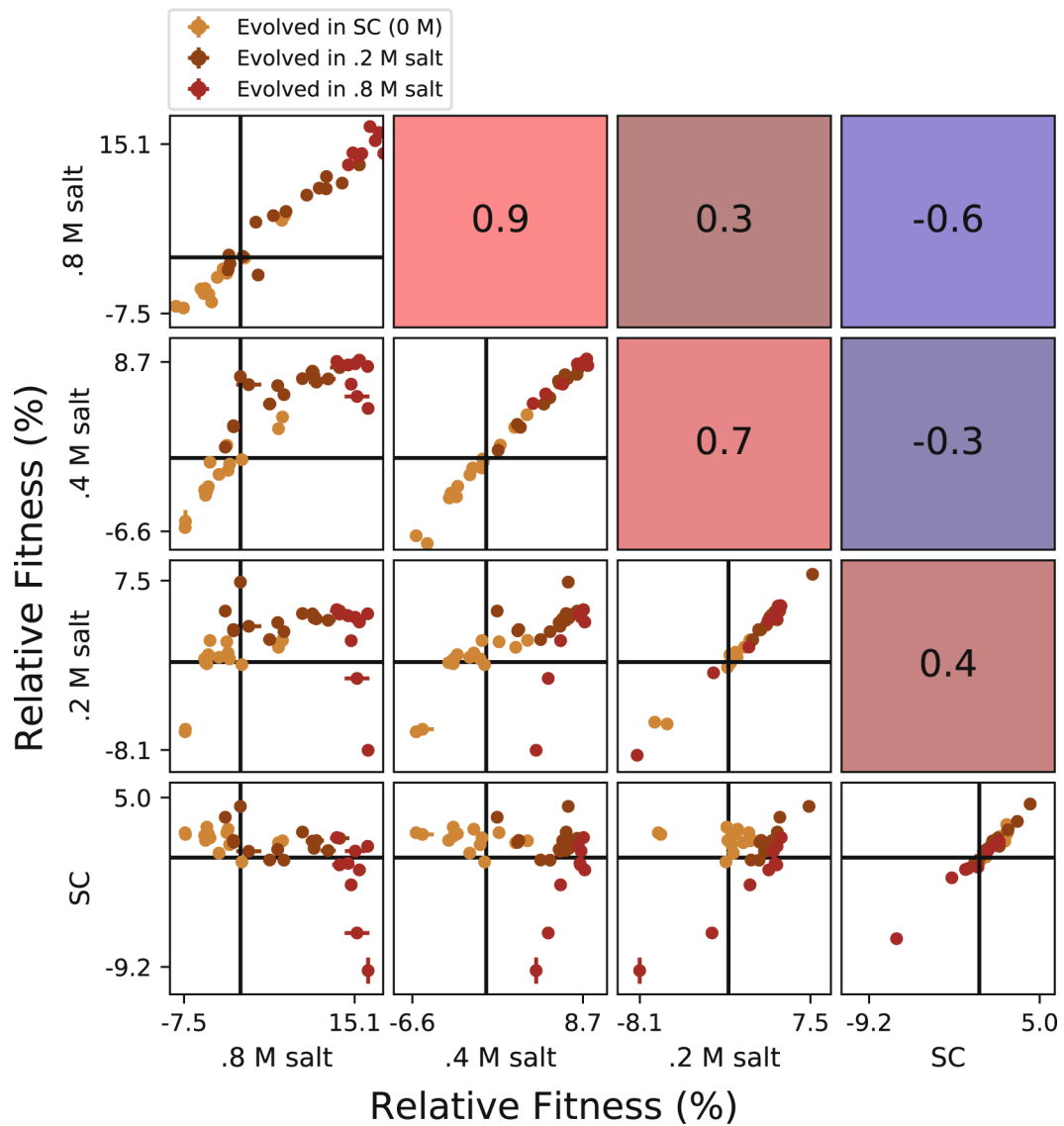
Extended Data Fig. 1 | Median fitness gains and losses, restricted to V^+ clones. Median fitness gains and losses among groups of clones from the same home environment, excluding V^- clones. Notations as in Fig. 1.



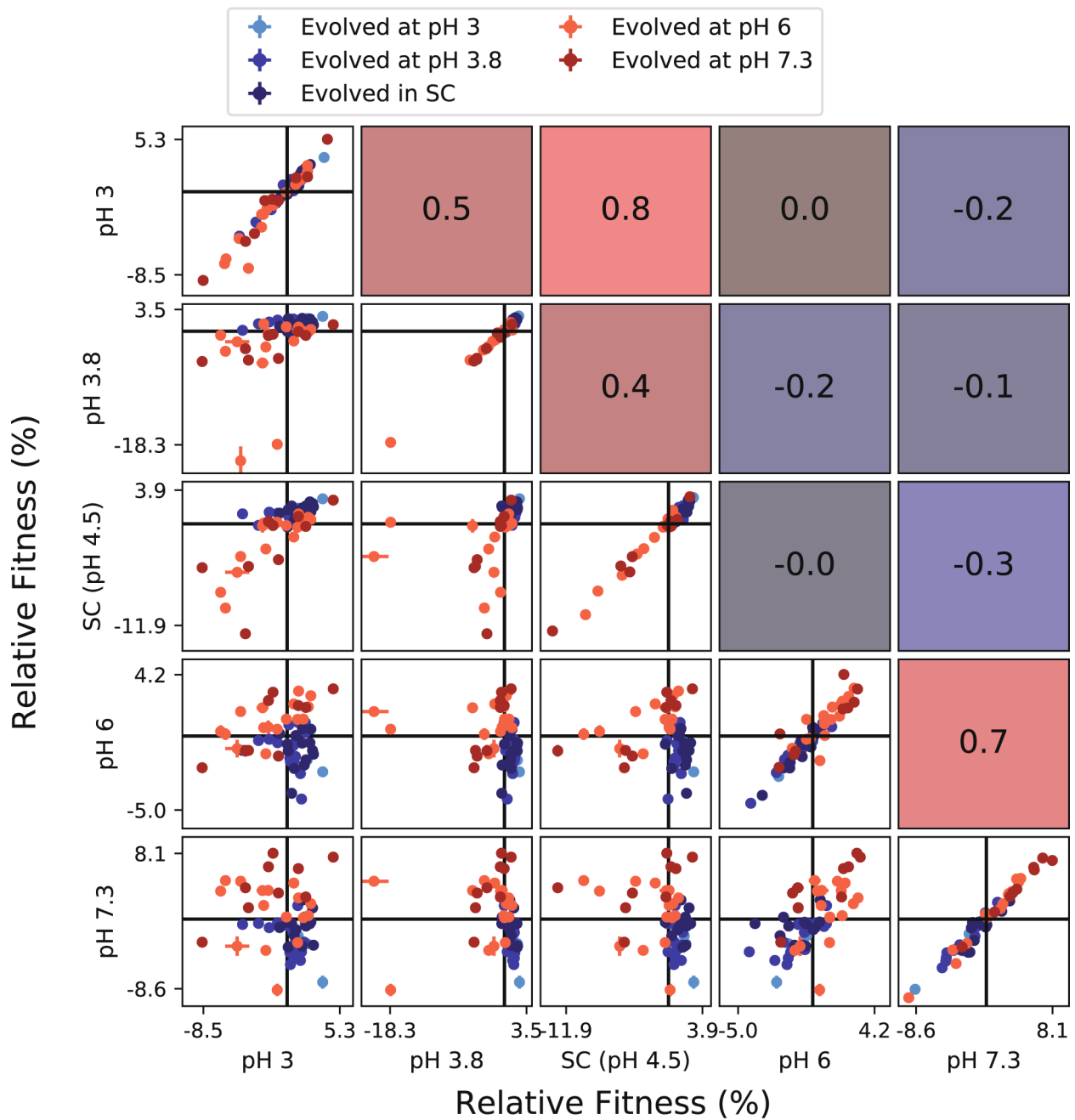
Extended Data Fig. 2 | Frequency-dependence of competition between V^+ and V^- . Fitness of a V^- clone relative to the ancestor at Low Temp, initiated at different initial frequencies. The frequency dependence of the relative fitness suggests that the fitness defect might be caused by a direct interaction between the competitors. Error bars show ± 1 s.e.m.



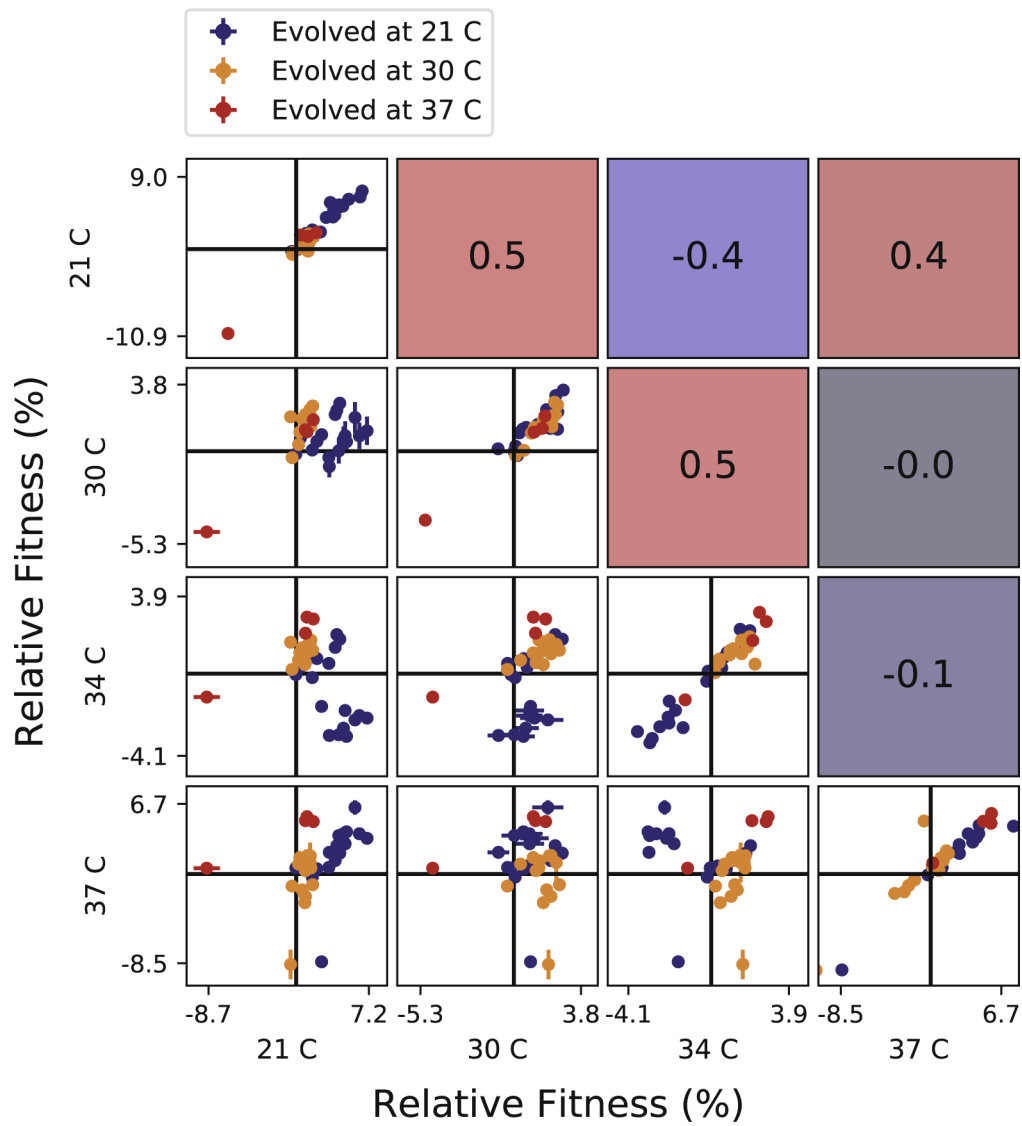
Extended Data Fig. 3 | Variance in fitness across environmental panels. As in Fig. 5a-c, but variance in fitness across groups of clones rather than means. Error bars represent ± 1 standard error of the variance.



Extended Data Fig. 4 | Correlations between clone fitness in different salt conditions. Each panel below the diagonal shows clone fitness in a particular pair of environments. (Error bars: ± 1 s.e.m. on clone fitness.) The diagonal shows the correlation between technical replicates in the fitness assay in each condition. Panels above the diagonal are colored by and display the Pearson correlation coefficient between clone fitness in the corresponding pair of environments.



Extended Data Fig. 5 | Correlations between clone fitness in different pH conditions. Each panel below the diagonal shows clone fitness in a particular pair of environments. (Error bars: ± 1 s.e.m. on clone fitness.) The diagonal shows the correlation between technical replicates in the fitness assay in each condition. Panels above the diagonal are colored by and display the Pearson correlation coefficient between clone fitness in the corresponding pair of environments.



Extended Data Fig. 6 | Correlations between clone fitness in different temperature conditions. Each panel below the diagonal shows clone fitness in a particular pair of environments. (Error bars: ± 1 s.e.m. on clone fitness.) The diagonal shows the correlation between technical replicates in the fitness assay in each condition. Panels above the diagonal are colored by and display the Pearson correlation coefficient between clone fitness in the corresponding pair of environments.

Reporting Summary

Nature Research wishes to improve the reproducibility of the work that we publish. This form provides structure for consistency and transparency in reporting. For further information on Nature Research policies, see [Authors & Referees](#) and the [Editorial Policy Checklist](#).

Statistics

For all statistical analyses, confirm that the following items are present in the figure legend, table legend, main text, or Methods section.

n/a Confirmed

- | | | |
|-------------------------------------|-------------------------------------|--|
| <input type="checkbox"/> | <input checked="" type="checkbox"/> | The exact sample size (n) for each experimental group/condition, given as a discrete number and unit of measurement |
| <input type="checkbox"/> | <input checked="" type="checkbox"/> | A statement on whether measurements were taken from distinct samples or whether the same sample was measured repeatedly |
| <input type="checkbox"/> | <input checked="" type="checkbox"/> | The statistical test(s) used AND whether they are one- or two-sided
<i>Only common tests should be described solely by name; describe more complex techniques in the Methods section.</i> |
| <input type="checkbox"/> | <input checked="" type="checkbox"/> | A description of all covariates tested |
| <input type="checkbox"/> | <input checked="" type="checkbox"/> | A description of any assumptions or corrections, such as tests of normality and adjustment for multiple comparisons |
| <input type="checkbox"/> | <input checked="" type="checkbox"/> | A full description of the statistical parameters including central tendency (e.g. means) or other basic estimates (e.g. regression coefficient) AND variation (e.g. standard deviation) or associated estimates of uncertainty (e.g. confidence intervals) |
| <input type="checkbox"/> | <input checked="" type="checkbox"/> | For null hypothesis testing, the test statistic (e.g. F , t , r) with confidence intervals, effect sizes, degrees of freedom and P value noted
<i>Give P values as exact values whenever suitable.</i> |
| <input checked="" type="checkbox"/> | <input type="checkbox"/> | For Bayesian analysis, information on the choice of priors and Markov chain Monte Carlo settings |
| <input checked="" type="checkbox"/> | <input type="checkbox"/> | For hierarchical and complex designs, identification of the appropriate level for tests and full reporting of outcomes |
| <input type="checkbox"/> | <input checked="" type="checkbox"/> | Estimates of effect sizes (e.g. Cohen's d , Pearson's r), indicating how they were calculated |

Our web collection on [statistics for biologists](#) contains articles on many of the points above.

Software and code

Policy information about [availability of computer code](#)

Data collection

Data analysis

For manuscripts utilizing custom algorithms or software that are central to the research but not yet described in published literature, software must be made available to editors/reviewers. We strongly encourage code deposition in a community repository (e.g. GitHub). See the Nature Research [guidelines for submitting code & software](#) for further information.

Data

Policy information about [availability of data](#)

All manuscripts must include a [data availability statement](#). This statement should provide the following information, where applicable:

- Accession codes, unique identifiers, or web links for publicly available datasets
- A list of figures that have associated raw data
- A description of any restrictions on data availability

Data used to generate Figures 1,2, and 5 is available in Supplementary Table S1. Data used to generate Figure 3 is available in Supplementary Table S2. Data used to generate Figure 4 is available in Supplementary Tables S1 and S3. Code used for analysis and figure generation is available at <https://github.com/erjerison/pleiotropy>. The sequences reported in this paper have been deposited in the BioProject database (accession number PRJNA554163). All 213 strains are available from the corresponding authors upon request.

Field-specific reporting

Please select the one below that is the best fit for your research. If you are not sure, read the appropriate sections before making your selection.

- Life sciences Behavioural & social sciences Ecological, evolutionary & environmental sciences

For a reference copy of the document with all sections, see [nature.com/documents/nr-reporting-summary-flat.pdf](https://www.nature.com/documents/nr-reporting-summary-flat.pdf)

Life sciences study design

All studies must disclose on these points even when the disclosure is negative.

Sample size	No sample size calculation was performed. The number of independent populations evolved per environment was fixed based on the maximum feasible number.
Data exclusions	No data was excluded from analysis of fitness changes. Clones were excluded from sequence data analysis if they had less than 5x coverage.
Replication	The experiment was carried out with n=20 independently evolved populations per environment. Fitness measurements were performed in triplicate.
Randomization	All populations were founded from independently-picked clones from the same strain stock.
Blinding	Researchers were not blinded during the experiment and analysis.

Reporting for specific materials, systems and methods

We require information from authors about some types of materials, experimental systems and methods used in many studies. Here, indicate whether each material, system or method listed is relevant to your study. If you are not sure if a list item applies to your research, read the appropriate section before selecting a response.

Materials & experimental systems

n/a	Included in the study
<input checked="" type="checkbox"/>	<input type="checkbox"/> Antibodies
<input checked="" type="checkbox"/>	<input type="checkbox"/> Eukaryotic cell lines
<input checked="" type="checkbox"/>	<input type="checkbox"/> Palaeontology
<input checked="" type="checkbox"/>	<input type="checkbox"/> Animals and other organisms
<input checked="" type="checkbox"/>	<input type="checkbox"/> Human research participants
<input checked="" type="checkbox"/>	<input type="checkbox"/> Clinical data

Methods

n/a	Included in the study
<input checked="" type="checkbox"/>	<input type="checkbox"/> ChIP-seq
<input type="checkbox"/>	<input checked="" type="checkbox"/> Flow cytometry
<input checked="" type="checkbox"/>	<input type="checkbox"/> MRI-based neuroimaging

Flow Cytometry

Plots

Confirm that:

- The axis labels state the marker and fluorochrome used (e.g. CD4-FITC).
- The axis scales are clearly visible. Include numbers along axes only for bottom left plot of group (a 'group' is an analysis of identical markers).
- All plots are contour plots with outliers or pseudocolor plots.
- A numerical value for number of cells or percentage (with statistics) is provided.

Methodology

Sample preparation	Flow cytometry was used to determine the relative abundance of two yeast populations: ymCitrine+ and ymCitrine-. (Note that flow cytometry was used for analysis only, not sorting.) No flow cytometry plots are shown in the manuscript (this is why boxes 1-4 are unchecked).
Instrument	BD LSRFortessa, BD LSRII
Software	BD Diva software was used on the instruments. FlowJo was used for analysis
Cell population abundance	To estimate the fitness of a query strain relative to a reference strain, an initially 1:1 mixed culture of the two strains was subject to flow cytometry analysis at two time points separated by about 20 generations. At each time point, the relative abundance of

two cell populations (query, ymCitrine⁻, and reference, ymCitrine⁺) was estimated based on typically 10 to 50 thousand events.

Gating strategy

Gating of the two populations was performed manually in FlowJo for each sample in a two-dimensional plot of SSC vs ymCitrine.

Tick this box to confirm that a figure exemplifying the gating strategy is provided in the Supplementary Information.